NANO LETTERS

Letter

pubs.acs.org/NanoLett

Prediction of a Two-Dimensional Organic Topological Insulator

Z. F. Wang, Ninghai Su, and Feng Liu*

Department of Materials Science and Engineering, University of Utah, Salt Lake City, Utah 84112, United States

ABSTRACT: Topological insulators (TI) are a class of materials exhibiting unique quantum transport properties with potential applications in spintronics and quantum computing. To date, all of the experimentally confirmed TIs are inorganic materials. Recent theories predicted the possible existence of organic TIs (OTI) in two-dimensional (2D) organometallic frameworks. However, those theoretically proposed structures do not naturally exist and remain to be made in experiments. Here, we identify a recently experimentally made 2D organometallic framework, consisting of π-conjugated nickel-bis-dithiolene with a chemical formula $Ni_3C_{12}S_{12}$, which exhibits nontrivial topological states in both a Dirac band and a flat band, therefore confirming the existence of OTI.

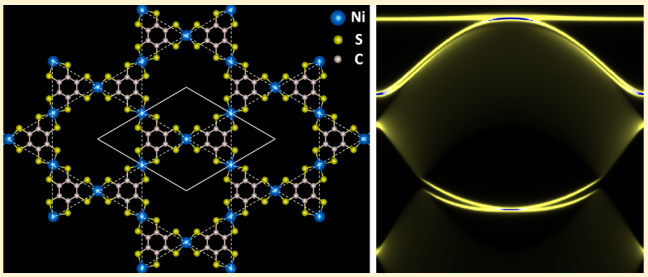

KEYWORDS: *Topological insulator, organometallic framework, Dirac band, flat band*

The concept of topological order in condensed matter physics provides a new perspective for understanding the origin of different quantum phases and has generated intense recent interest in searching for nontrivial topological materials, so-called topological insulators (TI).[1−13] The defining signature of a two-dimensional, 2D (3D), TI is its nontrivial bulk band topology around a global spin−orbit coupling (SOC) gap with corresponding topological edge (surface) states within the SOC gap. These characteristic edge (surface) states have a topological origin, which are protected from elastic back-scattering and localization, and hence hold potential for applications in spintronics and quantum computation devices. To date, all of the experimentally confirmed TIs are based on inorganic materials.[1−13] Recently, theories have predicted the possible existence of OTI in 2D organometallic frameworks,[14−16] but those theoretically proposed structures remain to be synthesized in the experiments.

In this work, we report the identification of nontrivial topological states in an experimental sample of 2D organometallic framework, $Ni_3C_{12}S_{12}$ lattice (Figure 1), recently synthesized by Kambe et al.[17] First-principles calculations of band structure, edge state, Chern number, and spin Hall conductance are performed to reveal the nontrivial topology in this lattice structure. A single-orbital tight-binding (TB) model is also given to illustrate its SOC gap opening mechanism.

First-principles calculations are carried out within the framework of the Perdew−Burke−Ernzerhof generalized gradient approximation using VASP.[18] All of the calculations are performed with a plane-wave cutoff of 500 eV on the 7 × 7 × 1 Monkhorst-Pack k-point mesh. The vacuum layer is 15 Å thick to ensure decoupling between neighboring slabs. During structural relaxation, all atoms are relaxed until the forces are smaller than 0.01 eV/Å.

Figure 1 shows the optimized 2D $Ni_3C_{12}S_{12}$ lattice structure, which adopts a kagome lattice. The optimized lattice constant is found to be L = 14.63 Å, in good agreement with the experimental value (14−15 Å).[17] Figure 2a shows the band structure of $Ni_3C_{12}S_{12}$ lattice with SOC around the Fermi level. We can clearly see that the typical kagome bands as shown previously in a TB model,[19] consisting of one flat band above two Dirac bands (top three red bands in Figure 2a, all of the bands are spin degenerated), which are well separated from the other black bands. Figure 2b shows the zoom-in band structures of the three kagome bands. The band gap of the Dirac band is Δ_1 = 13.6 meV, while the band gap between the flat band and the top branch of the Dirac band is Δ_2 = 5.8 meV. Both Δ_1 and Δ_2 vanish in the absence of SOC from the first-principles calculations.

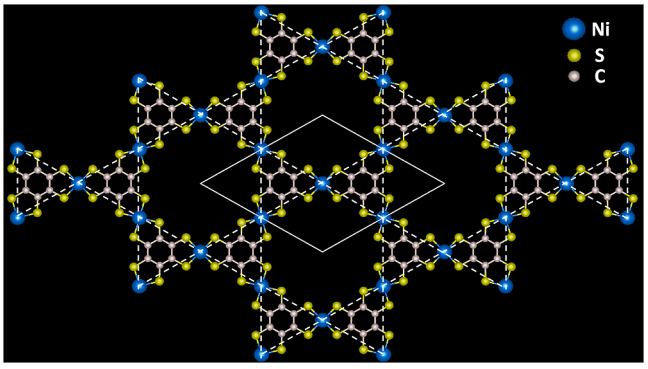

Figure 1. Atomic structure of the $Ni_3C_{12}S_{12}$ lattice. The solid lines show the unit cell, and the dashed lines outline the kagome lattice.

We then checked the edge states of the $Ni_3C_{12}S_{12}$ lattice, since the existence of topological edge states is an important

Received: March 30, 2013
Revised: May 10, 2013
Published: May 16, 2013

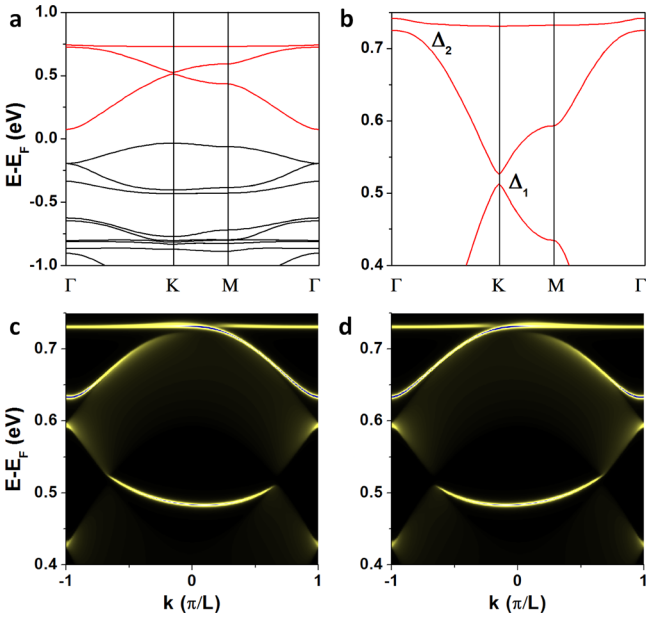

Figure 2. (a) 2D band structure of $Ni_3C_{12}S_{12}$ lattice along the high symmetry directions. (b) The zoom-in kagome bands around two SOC gaps. (c and d) The semi-infinite edge states for the spin-up and spin-down components, respectively. Overlapping c and d would give the 1D edge Dirac band in both SOC gaps as in Figure 4b.

signature of the 2D TIs. The edge states of the $Ni_3C_{12}S_{12}$ lattice is calculated by using the Wannier90 package,[20] in which a TB Hamiltonian in the basis of the maximally localized Wannier functions (MLWFs) is fitted to the first-principles band structures. Using these MLWFs, the edge Green's function of the semi-infinite lattice is constructed using the recursive method,[21] and the local density of state (LDOS) of the edge is calculated. This method provides a direct connectivity between the edge states and the bulk states. The LDOS of a semi-infinite $Ni_3C_{12}S_{12}$ lattice is shown in Figure 2c and d for spin-up and spin-down components, respectively, where one can see the nontrivial topological edge states that connect the bulk states and form a 1D Dirac cone in both SOC gaps (Δ_1 and Δ_2). In addition, the spin-up and spin-down edge states have inverse group velocity, which will propagate along opposite directions along the edge, as required for the 2D TI states.

We stress that the kagome bands of the $Ni_3C_{12}S_{12}$ lattice represent a real material system that realizes the single-orbital TB model on a kagome lattice as proposed by Tang et al.[19] The corresponding model Hamiltonian in the reciprocal space can be expressed as follows:

$$H = \begin{pmatrix} E_0 & 2t_1\cos k_1 & 2t_1\cos k_2 \\ 2t_1\cos k_1 & E_0 & 2t_1\cos k_3 \\ 2t_1\cos k_2 & 2t_1\cos k_3 & E_0 \end{pmatrix} \pm i2\lambda_1 \begin{pmatrix} 0 & \cos k_1 & -\cos k_2 \\ -\cos k_1 & 0 & \cos k_3 \\ \cos k_2 & -\cos k_3 & 0 \end{pmatrix} \quad (1)$$

where $\vec{a}_1 = (L/2)\hat{x}$, $\vec{a}_2 = (L/2)[(\hat{x} + \sqrt{3}\hat{y})/2]$, $\vec{a}_3 = \vec{a}_2 - \vec{a}_1$, $k_n = \vec{k}\cdot\vec{a}_n$, and L is the lattice constant. E_0 is the on-site energy, t_1 is the nearest-neighbor hopping parameter, λ_1 is the nearest-neighbor intrinsic SOC, and +(−) refers to the spin-up (spin-down) bands. The corresponding fitting parameters for the $Ni_3C_{12}S_{12}$ lattice are E_0 = 0.59 eV, t_1 = −0.07 eV, and λ_1 = 0.0035 eV, which show very good agreement with the first-principles results (Figure 3a). The TB model analysis indicates

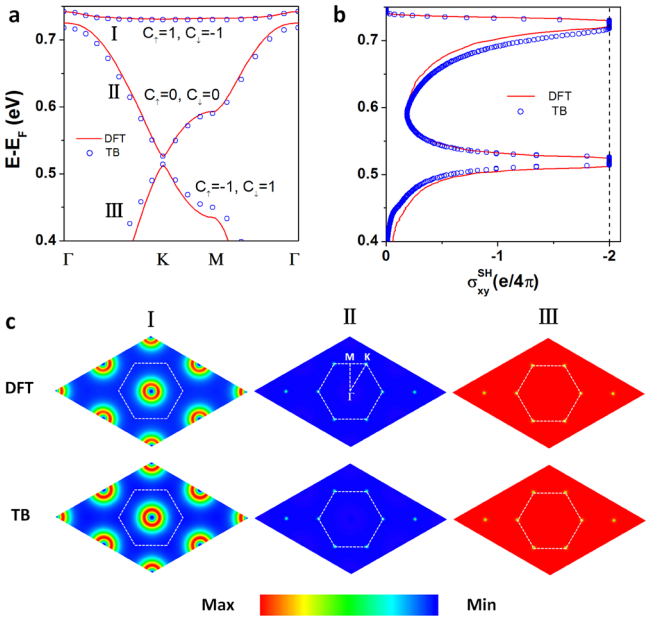

Figure 3. (a) A comparison between first-principles and single-orbital TB band structures for the flat (I) and Dirac (II and III) bands. (b) Same as a for the quantized spin Hall conductance within the energy window of the two SOC gaps. (c) Spin Berry curvatures in the reciprocal space for flat (left column) and Dirac bands (right two columns). The dashed lines mark the first Brillouin zone.

that the SOC gaps (Δ_1 and Δ_2) in the $Ni_3C_{12}S_{12}$ lattice are opened due to the intrinsic SOC of d-orbits of Ni atoms, given the inversion lattice symmetry that excludes the Rashba SOC effect.

To further confirm the nontrivial topology of the $Ni_3C_{12}S_{12}$ lattice, the Chern number (C) and spin Chern number (C^s) are calculated using the Kubo formula[22,23] as follows:

$$C = \frac{1}{2\pi}\int_{BZ} d^2\vec{k}\,\Omega(\vec{k})$$

$$\Omega(\vec{k}) = \sum_n f_n \Omega_n(\vec{k})$$

$$\Omega_n(\vec{k}) = -\sum_{n'\neq n} 2\mathrm{Im}\frac{\langle\psi_{nk}|v_x|\psi_{n',k}\rangle\langle\psi_{n',k}|v_y|\psi_{nk}\rangle}{(\varepsilon_{n',k} - \varepsilon_{nk})} \quad (2)$$

$$C^s = \frac{1}{2\pi}\int_{BZ} d^2\vec{k}\,\Omega^s(\vec{k})$$

$$\Omega^s(\vec{k}) = \sum_n f_n \Omega^s{}_n(\vec{k})$$

$$\Omega^s{}_n(\vec{k}) = -\sum_{n'\neq n} 2\mathrm{Im}\frac{\langle\psi_{nk}|j_x|\psi_{n',k}\rangle\langle\psi_{n',k}|v_y|\psi_{nk}\rangle}{(\varepsilon_{n',k} - \varepsilon_{nk})} \quad (3)$$

where n is the band index, ψ_{nk} is the eigenstate of eigenvalue ε_{nk} of band n, f_n is the Fermi distribution function, $v_{x/y}$ is the velocity operator, j_x is the spin current operator defined as $(s_z v_x$

dx.doi.org/10.1021/nl401147u | Nano Lett. 2013, 13, 2842−2845

+ $v_x s_z)/2$, and s_z is the spin operator. The Chern number and spin Chern number are defined as

$$C = C_\uparrow + C_\downarrow \qquad C^s = \frac{1}{2}(C_\uparrow - C_\downarrow) \tag{4}$$

From eqs 2−4, the Chern number of each band with different spins is calculated, as marked in Figure 3a. For both spins, the flat band and the bottom Dirac band have a nonzero Chern number (±1), while the top Dirac band has a zero Chern number. Thus, within the SOC gap of Δ_1 or Δ_2, the Chern number is zero, but the spin Chern number is −1, indicating that the $Ni_3C_{12}S_{12}$ lattice is topologically nontrivial.

The coexistence of two TI states, one from the Dirac band and the other from a flat band, at different energies can manifest in transport measurement. The spin Hall conductance can be obtained from the spin Chern number as

$$\sigma_{xy}^{SH} = \frac{e}{4\pi}(C_\uparrow - C_\downarrow) \tag{5}$$

Figure 3b shows the calculated spin Hall conductance as a function of energy using the first-principles and single-orbital TB method, which has a quantized value $(-2e/4\pi)$ within the energy window of both SOC gaps.

We also compare the calculated spin Berry curvature in Figure 3c, showing very good agreement between the first-principles method and the single-orbital TB model. The spin Berry curvature of the flat band is mainly around the Γ point (Figure 3c, left column), while that of the Dirac bands is around the K point (Figure 3c, right two columns). This again confirms that the $Ni_3C_{12}S_{12}$ lattice represents a real organometallic lattice to realize the original kagome model proposed by Tang et al.,[19] which has an interesting flat band with nonzero Chern number. By including many-body interactions in such nontrivial flat band, the fractional quantum Hall effect can also be realized.[24]

One distinct advantage of organic topological materials is their high tunability by using different metal atoms and molecular ligands. In addition to examining the experimentally made $Ni_3C_{12}S_{12}$ lattice, we also tested the $Au_3C_{12}S_{12}$ lattice by replacing Ni with Au to demonstrate the tunability of such lattices. The optimized lattice constant of $Au_3C_{12}S_{12}$ lattice is found to be L = 15.09 Å. Its band structure with SOC and semi-infinite edge states are shown in Figure 4a and b, respectively. Overall, the band structure and topology of the $Au_3C_{12}S_{12}$ lattice are physically same as those of the $Ni_3C_{12}S_{12}$ lattice, except that the Fermi level is now located in between the flat band and the Dirac point and the SOC gaps are larger with Δ_1 = 22.7 meV and Δ_2 = 9.5 meV.

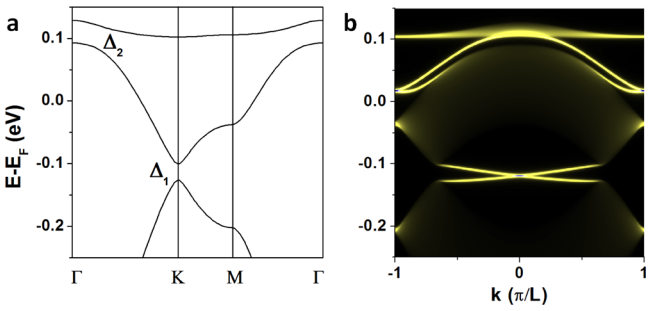

Figure 4. (a) Band structure of the $Au_3C_{12}S_{12}$ lattice. (b) The semi-infinite Dirac edge states (both spin up and spin down components) within the SOC gaps.

We note that the Fermi level is not in the SOC gaps in both lattices, so doping is needed. This requires doping one electron (or one hole) per unit cell in the $Au_3C_{12}S_{12}$ lattice and two (or four) electrons in the $Ni_3C_{12}S_{12}$ lattice, respectively, which corresponds to a doping concentration of $\sim 5 \times 10^{13}$ cm^{-2} to $\sim 2 \times 10^{14}$ cm^{-2}. In our first-principles calculations, the doping effect can be studied by removing (or adding) electrons from (or to) the lattice, and meanwhile adding a homogeneous background charge of opposite sign to maintain the system charge neutrality, as done before for other proposed OTIs.[14] In experiments, the doping effect can be achieved by the electrostatic gating. Recent experiment has demonstrated that the doping concentration in graphene can be achieved up to 4×10^{14} cm^{-2} for both electrons and holes by using a solid polymer electrolyte gate.[25]

Our predicted 2D OTI would offer several advantages over their inorganic counterparts. First, they should be less sensitive against oxidation, which would strongly simplify the device fabrication. Furthermore, the possibility to implement a wide variety of metal ions and organic ligands will enable specific tailoring of the electronic properties of OTI. Our recent work has already demonstrate such possibility to tune an OTI made of $Bi_2C_{18}H_{12}$ lattice into a magnetic OTI by substituting Bi with Mn atoms, and a quantum anomalous Hall effect having an odd Chern number is shown to be realizable in this magnetic OTI.[16] Therefore, it is reasonable to anticipate similar magnetic OTIs to be realized in the $Ni_3C_{12}S_{12}$ lattice by substituting Ni with other transition metal elements with large exchange energy.

In conclusion, using first-principles calculations, we identify a real OTI material in a recent experimentally synthesized 2D organometallic framework, which provides a viable approach for searching new TIs in organic materials. We envision that more OTIs will be discovered in the future, which will greatly broaden the scientific and technological impact of TIs.

AUTHOR INFORMATION

Corresponding Author

*E-mail: fliu@eng.utah.edu.

Notes

The authors declare no competing financial interest.

ACKNOWLEDGMENTS

This work was supported by NSF-MRSEC (Grant No. DMR-1121252). N.H.S. was supported by US DOE-BES (grant no. DE-FG02-04ER46148). Z.F.W. acknowledges additional support from ARL (Cooperative agreement no. W911NF-12-2-0023). We thank the CHPC at University of Utah and NERSC for providing the computing resources.

REFERENCES

(1) Hasan, M. Z.; Kane, C. L. *Rev. Mod. Phys.* **2010**, *82*, 3045.
(2) Qi, X.-L.; Zhang, S.-C. *Rev. Mod. Phys.* **2011**, *83*, 1057.
(3) Kane, C. L.; Mele, E. J. *Phys. Rev. Lett.* **2005**, *95*, 226801.
(4) Fu, L.; Kane, C. L. *Phys. Rev. B* **2007**, *76*, 045302.
(5) Bernevig, B. A.; Hughes, T. L.; Zhang, S.-C. *Science* **2006**, *314*, 1757.
(6) König, M.; Wiedmann, S.; Brüne, C.; Roth, A.; Buhmann, H.; Molenkamp, L. W.; Qi, X.-L.; Zhang, S.-C. *Science* **2007**, *318*, 766.
(7) Gehring, P.; Benia, H. M.; Weng, Y.; Dinnebier, R.; Ast, C. R.; Burghard, M.; Kern, K. *Nano Lett.* **2013**, *13*, 1179.

(8) Li, H.; Cao, J.; Zheng, W.; Chen, Y.; Wu, D.; Dang, W.; Wang, K.; Peng, H.; Liu, Z. *J. Am. Chem. Soc.* **2012**, *134*, 6132.
(9) Müchler, L.; Zhang, H.; Chadov, S.; Yan, B.; Casper, F.; Kübler, J.; Zhang, S.-C.; Felse, C. *Angew. Chem., Int. Ed.* **2012**, *51*, 7221.
(10) Liu, Z.; Liu, C.-X.; Wu, Y.-S.; Duan, W.-H.; Liu, F.; Wu, J. *Phys. Rev. Lett.* **2011**, *107*, 136805.
(11) Yang, F.; Miao, L.; Wang, Z. F.; Yao, M.-Y.; Zhu, F.; Song, Y. R.; Wang, M.-X.; Xu, J.-P.; Fedorov, A. V.; Sun, Z.; Zhang, G. B.; Liu, C.; Liu, F.; Qian, D.; Gao, C. L.; Jia, J.-F. *Phys. Rev. Lett.* **2012**, *109*, 016801.
(12) Miao, L.; Wang, Z. F.; Ming, W.-M.; Yao, M.-Y.; Wang, M.-X.; Yang, F.; Zhu, F.; Fedorov, A. V.; Sun, Z.; Gao, C. L.; Liu, C.; Xue, Q.-K.; Liu, F.; Qian, D.; Jia, J.-F. *Proc. Natl. Acad. Sci. U.S.A.* **2013**, *110*, 2758.
(13) Wang, Z. F.; Yao, M.-Y.; Ming, W.-M.; Miao, L.; Zhu, F.; Liu, C.; Gao, C. L.; Qian, D.; Jia, J.-F.; Liu, F. *Nat. Commun.* **2013**, *4*, 1384.
(14) Wang, Z. F.; Liu, Z.; Liu, F. *Nat. Commun.* **2013**, *4*, 1471.
(15) Liu, Z.; Wang, Z. F.; Mei, J.-W.; Wu, Y.; Liu, F. *Phys. Rev. Lett.* **2013**, *110*, 106804.
(16) Wang, Z. F.; Liu, Z.; Liu, F. *Phys. Rev. Lett.* **2013**, *110*, 196801.
(17) Kambe, T.; Sakamoto, R.; Hoshiko, K.; Takada, K.; Miyachi, M.; Ryu, J.-H.; Sasaki, S.; Kim, J.; Nakazato, K.; Takata, M.; Nishihara, H. *J. Am. Chem. Soc.* **2013**, *135*, 2462.
(18) Kresse, G.; Hafner, J. *Phys. Rev. B* **1993**, *47*, 558.
(19) Tang, E.; Mei, J.-W.; Wen, X.-G. *Phys. Rev. Lett.* **2011**, *106*, 236802.
(20) Mostofi, A. A.; Yates, J. R.; Lee, Y.-S.; Souza, I.; Vanderbilt, D.; Marzari, N. *Comput. Phys. Commun.* **2008**, *178*, 685.
(21) Sancho, M. P. L.; Sancho, J. M. L.; Sancho, J. M. L.; Rubio, J. *J. Phys. F* **1985**, *15*, 851.
(22) Yao, Y. G.; Kleinman, L.; MacDonald, A. H.; Sinova, J.; Jungwirth, T.; Wang, D.-S.; Wang, E.; Niu, Q. *Phys. Rev. Lett.* **2004**, *92*, 037204.
(23) Yao, Y. G.; Fang, Z. *Phys. Rev. Lett.* **2005**, *95*, 156601.
(24) Sheng, D. N.; Gu, Z.-C.; Sun, K.; Sheng, L. *Nat. Commun.* **2011**, *2*, 389.
(25) Efetov, D. K.; Kim, P. *Phys. Rev. Lett.* **2010**, *105*, 256805.